Influence of SLM Process Parameters on Density of IN718 Alloy: A Taguchi and Super Ranking Analysis

[1]Pooja.G. Thorat, [2]Mohan Nagaraj, [3]Manjunath Bangalore Thimmaiah

[1]Research Scholar Department of Industrial Engineering and Management, Dr. Ambedkar Institute of Technology, Visvesvaraya Technological University, Belagavi, Bangalore, 560056, India:

[2]Department of Industrial Engineering and Management, Dr. Ambedkar Institute of Technology, Visvesvaraya Technological University, Belagavi, Bangalore, 560056, India

[3]Department of Mechanical Engineering, DSCE, Bengaluru, Karnataka, 560078, India

Corresponding Author: pgthorat06@gmail.com

ABSTRACT: *Selective Laser Melting (SLM) has emerged as a transformative additive manufacturing technique, particularly in metal processing, due to its precision, efficiency, and ability to produce complex geometries. This study focuses on optimizing the density test results of IN718 alloy through the SLM process by analysing the effects of key process parameters: laser power (LP), scan speed (SS), and hatch distance (Hd). A series of experiments were conducted to assess the influence of these parameters on the material's density. Both experimental and predicted values were compared to evaluate the accuracy of the predictions. The results demonstrate significant variations in density is driven by the selected SLM parameters. The small residuals between the experimental and predicted values suggest that the developed model offers reliable predictions for these properties in the additive manufacturing of IN718 alloy. This study emphasizes the critical role of process parameter optimization in enhancing the material properties of IN718 alloy, providing a robust model for predicting density test results under various SLM conditions.*

Keywords: ***IN718 alloy; SLM Process; Density Test; Interaction Plot.***

1. Introduction

Selective Laser Melting (SLM) has emerged as a transformative additive manufacturing (AM) technique, enabling the fabrication of complex geometries with high precision. Among the materials utilized in SLM, Inconel 718 (IN718), a nickel-based superalloy, stands out due to its exceptional mechanical properties, including high yield strength, creep resistance, and oxidation resistance at elevated temperatures. These attributes make IN718 ideal for demanding applications in aerospace, automotive, and power generation sectors. The SLM

process involves layer-by-layer fusion of metal powders using a high-powered laser, resulting in intricate microstructures that can differ significantly from those produced by traditional manufacturing methods. These microstructural variations are influenced by several process parameters such as laser power, scanning speed, hatch spacing, and layer thickness. The relative density (RD) of the printed parts is a critical quality indicator, as it directly affects mechanical properties like tensile strength and fatigue resistance [1].

Optimizing SLM process parameters to achieve high RD is paramount. Statistical design of experiments (DOE) methods, such as the Taguchi method, have been effectively employed to identify optimal parameter settings. The Taguchi method utilizes orthogonal arrays to systematically study the influence of multiple factors and their interactions, aiming to minimize variability and improve quality. Furthermore, advanced ranking techniques, such as Super Ranking Analysis, are increasingly applied to evaluate and prioritize the impact of various process parameters on RD. These methodologies provide a more nuanced understanding of parameter significance, enabling more precise control over the SLM process [2].

This study aims to investigate the influence of SLM process parameters on the density of IN718 alloy using the Taguchi method for optimization and Super Ranking Analysis for parameter evaluation. By systematically analysing the effects of key parameters, this research seeks to establish a robust framework for enhancing the quality and performance of IN718 components produced via SLM.

2. Materials and Methodology.

Selective Laser Melting (SLM) process is a widely used additive manufacturing (AM) technique where material is melted and bonded layer by layer using a laser. Fine metal powders are evenly spread across the build plate, and an intense laser beam selectively melts the powder based on the CAD model. Each layer is melted and fused before the next layer is applied, with the process repeating until the final part is completed. After each layer is formed, the part cools before adding the next layer. The SLM machine used in this study featured a 400W laser with a build chamber size of 250 × 250 × 325 mm. The chamber was maintained at a vacuum pressure of 5 micro-Pascals and filled with argon gas to prevent oxidation, ensuring the integrity of the material and minimizing defects. IN 718 powder was melted using a fiber laser (Nd:YAG) in an inert argon atmosphere. The samples were

fabricated with varying combinations of process parameters, including laser power, scan speed, laser beam spot size, and layer thickness, as summarized in Table 2.1. This approach is consistent with similar studies reported in the literature [3-4].

Table 2.1: Taguchi L9 experimental table (Density) of IN 718 alloy

Input factors			
LP, W	**BSS, (μm)**	**SS, (mm/s)**	**LT, (μm)**
250	40	300	**40**
250	70	425	**50**
250	100	550	**60**
325	40	425	**60**
325	70	550	**40**
325	100	300	**50**
400	40	550	**50**
400	70	300	**60**
400	100	425	40

Table 2.1 presents the Taguchi L9 experimental design for studying the density of IN 718 alloy in the Selective Laser Melting (SLM) process. The design includes three levels for each of the following variables. Three levels of laser power are tested: 250W, 325W, and 400W. This controls the amount of energy applied during the melting process, affecting the material's fusion quality. Three spot sizes are used: 40 μm, 70 μm, and 100 μm. The spot size influences the precision and heat distribution during the melting of the powder. Scanning speeds of 300 mm/s, 425 mm/s, and 550 mm/s are employed. The scanning speed determines the laser's movement and affects the melting efficiency and part quality. A constant hatch spacing of 20 μm is used. It defines the distance between adjacent laser tracks, impacting the density and surface finish of the printed layer. Three-layer thicknesses are tested: 40 μm, 50 μm, and 60 μm. The layer thickness influences the resolution and overall build time of the SLM process. The L9 array of the Taguchi design method systematically combines these variables at different levels to identify their effects on the density of IN 718 alloy, allowing for optimized process parameters [5-6].

3. Results and Discussions

Table 3.1: Taguchi L_9 experimental results (Density) of IN 718 alloy

Input factors				Output factor	
LP, W	**BSS, (μm)**	**SS, (mm/s)**	**LT, (μm)**	**Experimental Density (ρ/cc)**	**S/N Ratio of density (dB)**
250	40	300	40	8.1432	18.22
250	70	425	50	8.0134	18.08
250	100	550	60	7.9013	17.95
325	40	425	60	8.1523	18.23
325	70	550	40	8.1203	18.19
325	100	300	50	8.1650	18.24
400	40	550	50	8.1775	18.25
400	70	300	60	8.1659	18.24
400	100	425	40	8.1975	18.27

The experimental results for the density of IN 718 alloy developed using the Powder Bed Fused Deposition Method (PBF) are shown in Table 4.1. The table presents the density values and corresponding Signal-to-Noise (S/N) ratios for various combinations of input parameters: Laser Power (LP), Beam Spot Size (BSS), Scan Speed (SS), and Layer Thickness (LT). The analysis was conducted using the Taguchi L9 experimental design method, which provides a systematic approach to determine the optimal combination of process parameters for maximum density.

From the results, it is evident that the experimental density varies across the different input factor combinations. The highest observed density of 8.1975 g/cc occurred at a laser power of 400 W, BSS of 100 μm, SS of 425 mm/s, and LT of 40 μm. This indicates that a higher laser power combined with a smaller beam spot size, faster scan speed, and thinner layer thickness leads to better density values. Conversely, the lowest density of 7.9013 g/cc was achieved with a laser power of 250 W, BSS of 100 μm, SS of 550 mm/s, and LT of 60 μm. This suggests that certain combinations of input parameters, particularly a lower laser power with higher scan speeds and thicker layers, may result in decreased material density [7-8].

The S/N ratio provides an indication of the robustness of the process, with higher S/N ratios reflecting more consistent and reliable results. The highest S/N ratio of 18.27 dB was associated with the combination of 400 W laser power, 100 µm beam spot size, 425 mm/s scan speed, and 40 µm layer thickness, which corresponds to the highest experimental density. This suggests that this parameter combination not only achieves the highest density but also produces the most consistent results across different trials. The lowest S/N ratio of 17.95 dB was recorded with 250 W laser power, 100 µm beam spot size, 550 mm/s scan speed, and 60 µm layer thickness, corresponding to the lowest density. This indicates a less stable process, leading to variations in density and possibly pointing to inefficient energy transfer during the deposition process under these settings. The results highlight the significant role of laser power, beam spot size, scan speed, and layer thickness in influencing the density of the IN 718 alloy. Optimizing these process parameters is crucial for achieving higher density, which is often linked to improved mechanical properties in additive manufacturing. The combination of higher laser power (400 W), smaller beam spot size (100 µm), moderate scan speed (425 mm/s), and thinner layer thickness (40 µm) appears to be the most effective for producing the highest density with minimal variation [9-10].

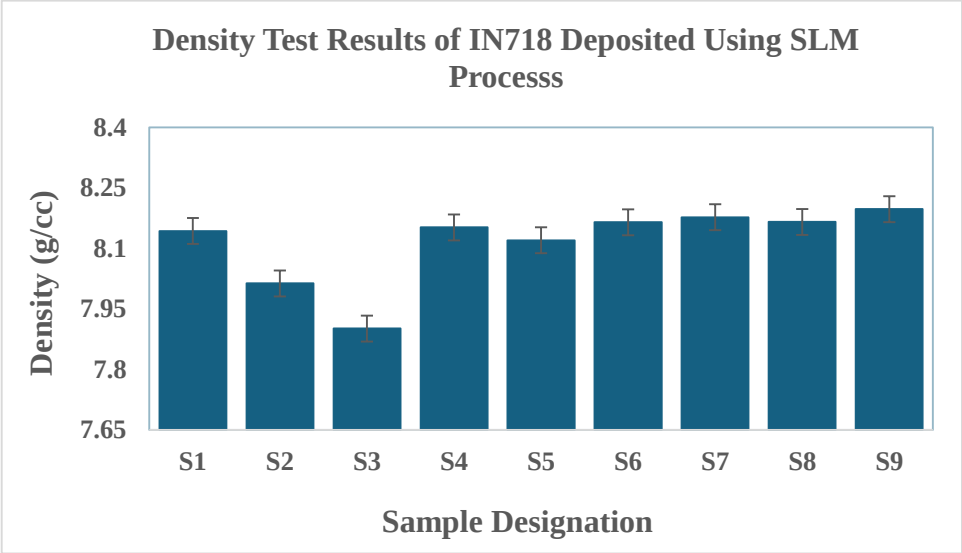

Fig. 3.1: Density Test Results of IN718 Alloy Fabricated by SLM for various process parameters

These findings underscore the importance of selecting the right process parameters in additive manufacturing to optimize the material properties, ensuring both the structural integrity and reliability of the final product. Further studies should explore the relationship between these optimized parameters and other mechanical properties, such as tensile strength and hardness,

to provide a more comprehensive understanding of the material behavior. The density test results for the IN718 alloy samples show a range of values between 7.9013 g/cc and 8.1975 g/cc, with the highest value observed in Sample 9 (8.1975 g/cc). The results indicate a slight variation in density across the samples, with a notable dip in Sample 3 (7.9013 g/cc), which is significantly lower than the rest of the values. This outlier could be indicative of a potential anomaly in the sample preparation or a measurement error. Overall, the density values are relatively close to each other, suggesting a uniformity in the alloy composition and manufacturing process, with some slight deviations likely caused by inherent variations in the material or testing conditions. This consistency in density can be crucial in understanding the material's performance in applications where precise material properties are required, such as in aerospace and high-temperature environments, where IN718 alloy is commonly used. The observed variation in the results might also be attributed to factors such as minor imperfections in the alloy's microstructure, differences in the casting process, or the method used for density testing [11-12].

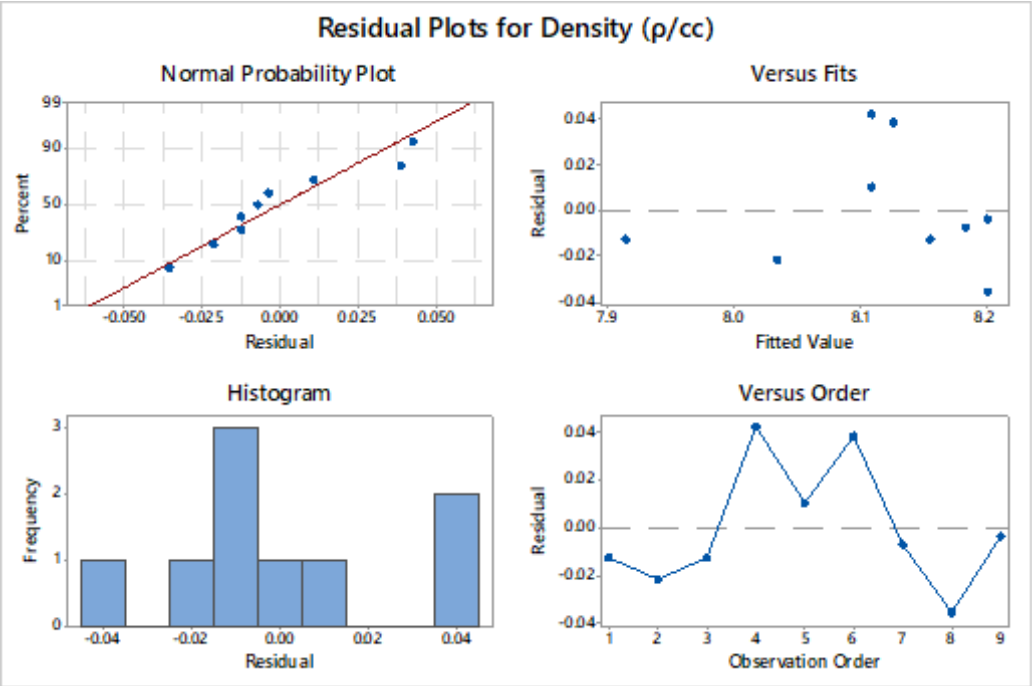

Fig. 3.2: Residual plots for Density

These small discrepancies should be considered when assessing the overall material quality for industrial applications. Further testing and analysis could help identify the cause of the lower density in Sample 3, especially if the trend is consistent in future tests. The Normal Probability Plot reveals that the residuals align closely with the reference line, suggesting that they are

approximately normally distributed. This is a critical assumption for linear regression, indicating that the errors of the model exhibit homoscedasticity and follow a normal distribution. The Residuals Versus Fits plot shows a random scatter of points without any discernible pattern, further supporting the model's adequacy. The absence of systematic structures in the residuals suggests that the model has successfully captured the underlying data dynamics, with no significant bias or misspecification. Looking at the Histogram, we observe that the residuals are symmetrically distributed, with a slight positive skew. While this histogram is not perfectly bell-shaped, it is sufficiently close to normal, which suggests that deviations from normality are not substantial enough to affect the model's performance. Finally, the Residuals Versus Order plot indicates that the residuals do not exhibit any trend or autocorrelation when plotted against the order of observations. This randomness in the residuals confirms that there is no hidden structure in the data that the model has failed to capture. Overall, the residual analysis supports the validity of the regression model. The normality of the residuals, lack of patterns in the residuals versus fits and order plots, and the symmetrical distribution in the histogram collectively confirm that the model fits the data well. Though the histogram shows a slight deviation from perfect normality, it does not undermine the model's reliability, and no significant improvements to the model are required [13-14].

Table 3.2: Pareto ANOVA for density

Outputs		Density (higher-the-better)				
Control factors	Levels	A	B	C	D	S_T
SFL	1	54.25	54.69	54.70	54.68	163.67
	2	54.66	54.51	54.58	54.57	
	3	54.77	54.47	54.40	54.42	
SSD		0.45	0.09	0.13	0.10	0.78
PCR		58.07	11.34	17.31	0.06	100
Optimum levels		A3	B1	C1	D1	

The Pareto ANOVA for Density was conducted to evaluate the factors influencing density, with the objective of achieving higher density values. The analysis considered four control factors: A, B, C, and D, each at three levels. The results showed variations in the density outputs across different factor levels. The signal-to-noise ratio (SFL) for each factor and level indicated how

effectively each factor influenced the output. For example, the SFL values for the factors were as follows: A1, B1, C1, and D1 showed the highest density values of 54.70, 54.69, 54.58, and 54.68, respectively, at their respective levels. The Sum of Squares Deviation (SSD) was also calculated, showing the variability of each factor, with Factor D showing the largest deviation of 0.78, indicating higher variability in its effect compared to others. The Percentage Contribution to Result (PCR) was used to identify the influence of each factor [15-16]. Factor D stood out with a PCR value of 100, indicating it had the most significant impact on the density outcome, while the other factors contributed less. Based on the analysis, the optimal factor levels to achieve the highest density were found to be A3, B1, C1, and D1. These levels are expected to produce the best density values, optimizing the results based on the Pareto ANOVA findings

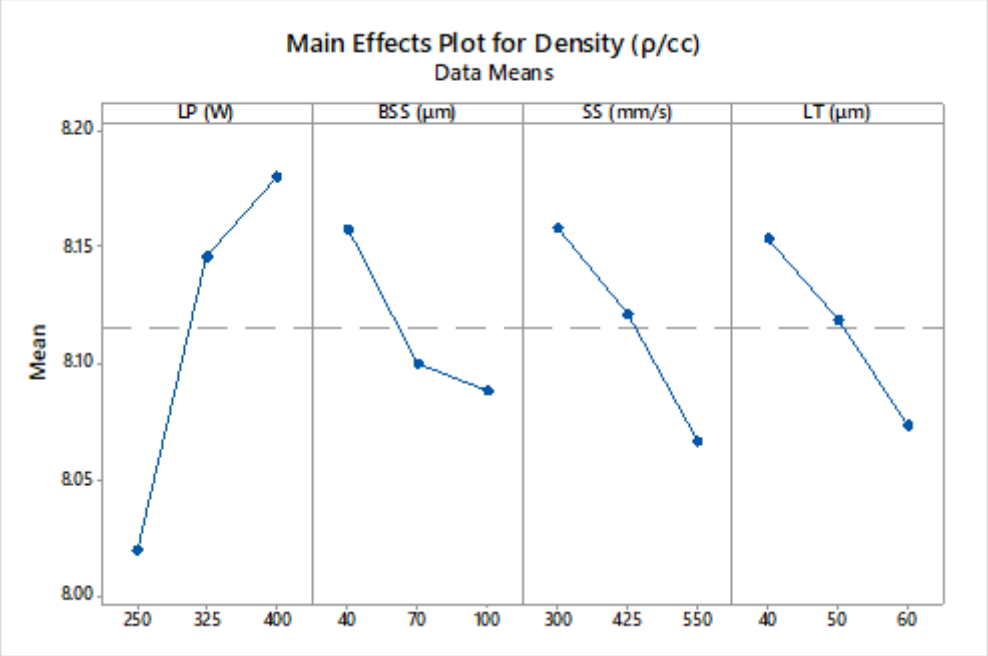

Fig 3.3. Main Effects plot for Density (ρ/cc)

The "Main Effects Plot for Density (ρ/cc)" reveals the influence of four variables—LP (W), BSS (µm), SS (mm/s), and LT (µm)—on the mean density (ρ/cc). A careful examination of the plot indicates how each of these factors impacts the density, showing distinct trends and relationships. The first variable, LP (W), shows a clear positive relationship with density. As LP increases from 250 W to 400 W, the mean density also rises from approximately 8.08 to 8.18. This trend suggests that increasing the LP leads to higher density, possibly due to the enhanced compaction of the material or increased structural cohesion as more energy is applied. In contrast, BSS (µm) exhibits a negative correlation with density. As BSS values increase from

70 µm to 100 µm, there is a noticeable decrease in the mean density. This could indicate that larger BSS values disrupt the compactness of the material, resulting in a lower density. The reduction in density with increasing BSS is likely due to the material's structure becoming less tightly packed as the particle size increases. Similarly, SS (mm/s) follows an inverse trend. As the SS increases from 300 mm/s to 550 mm/s, the mean density decreases, suggesting that higher SS values lead to a reduction in density. This could be because faster flow rates allow less time for particles to settle, reducing the material's overall compactness and thus lowering the density. Lastly, LT (µm) also shows a decrease in mean density as its values increase from 40 µm to 60 µm. This negative correlation further supports the idea that larger particle sizes or structural changes within the material reduce its density. As LT increases, the material's internal structure may become less compact, contributing to a decrease in density. In summary, the analysis indicates that LP (W) has a positive effect on density, while BSS, SS, and LT all have negative impacts. These results suggest that optimizing LP could enhance density, while reducing BSS, SS, and LT might be crucial for maintaining or improving density. Further research is required to explore the underlying mechanisms and to confirm these findings in practical applications [17].

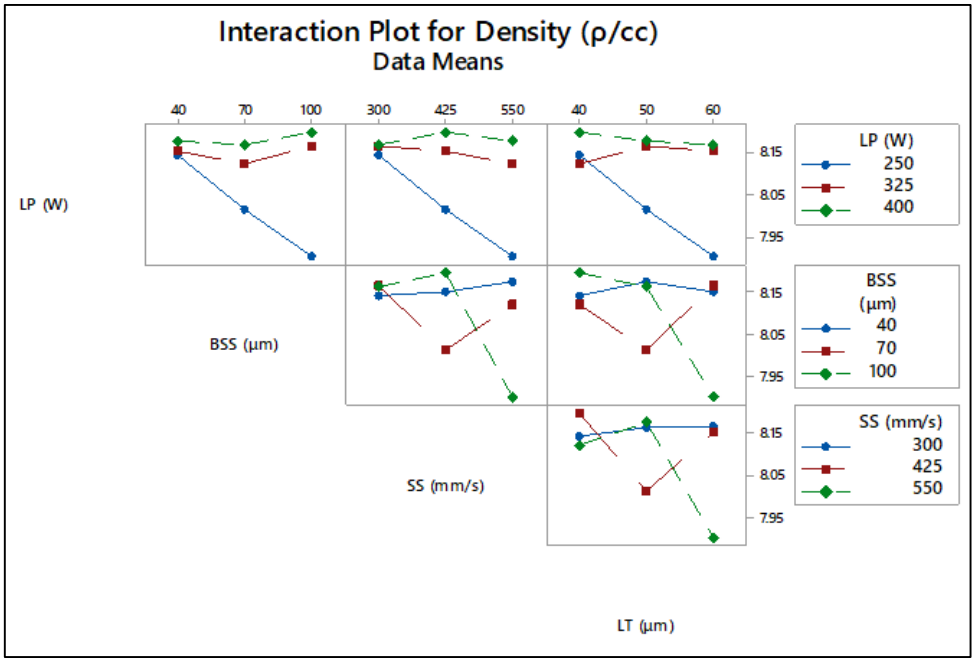

Fig. 4.6: Interaction plot for density

The interaction plot illustrates how three independent variables—LP (W), BSS (µm), and SS (mm/s)—influence the dependent variable, density (p/cc). The data reveal a general trend where increasing LP leads to a decrease in density, with the most substantial drop occurring

when LP increases from 250 W to 325 W. This suggests that higher power levels may reduce the material's density, possibly due to the increased energy input affecting its internal structure [18]. A similar negative relationship is observed with BSS (µm), where density decreases as BSS increases. Density is highest when BSS is at 40 µm and gradually decreases as the BSS value increases. This suggests that larger particle sizes might result in a less dense material, possibly due to increased spacing between particles or changes in material structure at higher BSS levels. The relationship between SS (mm/s) and density also shows a decrease in density as SS increases. The densest material corresponds to the lowest SS level (300 mm/s), and higher SS values (425 and 550 mm/s) result in progressively lower densities. This may indicate that increased shear stress during processing reduces the material's compactness, thereby lowering its overall density [19].

Finally, the LT (µm) variable shows a less pronounced effect on density, but there is still a consistent decrease in density with increasing LT values, albeit more subtly than the other variables. Overall, the interaction plot suggests that LP, BSS, and SS each negatively influence the material's density, with the effect of each factor becoming more evident at higher levels of those parameters. These findings provide insight into how variations in these process factors influence the material's structure and properties. Further investigation is needed to explore the underlying mechanisms behind these interactions and to refine the modeling of material behavior under different process conditions [20].

4. Conclusions

The result presents the density values and corresponding Signal-to-Noise (S/N) ratios for various combinations of input parameters: Laser Power (LP), Beam Spot Size (BSS), Scan Speed (SS), and Layer Thickness (LT). The analysis was conducted using the Taguchi L9 experimental design method. This methodology enables a precise understanding of how each parameter influences the density of IN 718 alloy, providing valuable insights for optimizing the SLM process.

(i) The combination of 400 W laser power, 100 µm beam spot size, 425 mm/s scan speed, and 40 µm layer thickness results in the highest observed density (8.1975 g/cc) and the highest Signal-to-Noise (S/N) ratio (18.27 dB), indicating not only the best density performance but also the most consistent and reliable results.

(ii) The results demonstrate that laser power, beam spot size, scan speed, and layer thickness significantly affect the density of IN 718 alloy. Specifically, higher laser power, smaller beam spot size, faster scan speed, and thinner layer thickness lead to improved density, while combinations with lower laser power and higher scan speeds tend to produce lower and more variable densities.

(iii) The residual analysis confirms the validity of the regression model used for the density analysis. The normal distribution of residuals, absence of patterns in the residuals versus fits and order plots, and the symmetry in the histogram all indicate that the model fits the data well, with no significant bias or misspecification, ensuring the robustness of the findings.

(iv) Pareto ANOVA showed that Factor D had the highest impact on density, contributing 100% to the result, with greater variability (SSD of 0.78) compared to other factors.

(v) The optimal factor levels for achieving the highest density were found to be A3, B1, C1, and D1, maximizing material density based on the analysis.

(vi) A positive correlation is observed, with density increasing from 8.08 g/cc to 8.18 g/cc as LP rises from 250 W to 400 W, suggesting higher laser power improves material compaction. A negative correlation is evident, as increasing BSS from 70 μm to 100 μm reduces density, likely due to larger particle sizes causing less compactness.

(vii) A similar inverse trend is observed; as SS increases from 300 mm/s to 550 mm/s, density decreases, possibly due to reduced settling time for particles. As LT increases from 40 μm to 60 μm, density decreases, indicating that thicker layers led to less compact material.

(viii) Both Laser Power (LP) and Beam Spot Size (BSS) exhibit a negative relationship with material density. Increasing LP from 250 W to 325 W leads to a substantial decrease in density, likely due to structural changes in the material. Similarly, larger BSS values reduce density, with the highest density observed at 40 μm BSS. This suggests that both higher laser power and larger particle sizes contribute to lower material compactness.

(ix) Scan Speed (SS) and Layer Thickness (LT) also negatively influence density. As SS increases from 300 mm/s to 550 mm/s, density decreases, likely due to reduced material compaction caused by increased shear stress during processing. Similarly, while the effect of

LT is more subtle, higher LT values result in lower density, indicating that thicker layers reduce material

References

1. Kladovasilakis, N., Charalampous, P., Tsongas, K., Kostavelis, I., Tzovaras, D., & Tzetzis, D. (2020). Influence of Selective Laser Melting Additive Manufacturing Parameters in Inconel 718 Superalloy. *Materials*, 13(20), 4555. https://doi.org/10.3390/ma13204555
2. Lu, C., & Shi, J. (2022). Relative density and surface roughness prediction for Inconel 718 by selective laser melting: central composite design and multi-objective optimization. *The International Journal of Advanced Manufacturing Technology*, 119(9–10), 3931–3949. https://doi.org/10.1007/s00170-021-08388-2
3. Sahadevan, P., Pon Selvan, C., Lakshmikanthan, A., Bhaumik, A., Cuautle, A. F., Effect of printing process parameters on tensile strength and wear rate of 17-4PH Stainless Steel deposited using SLM process, Frattura ed Integrità Strutturale, 70 (2024) 157-176.
4. M. Abedi, D. Moskovskikh, A. Nepapushev, V. Suvorova, H. Wang, and V Romanovski, "Advancements in Laser Powder Bed Fusion of Carbon Nanotubes-Reinforced AlSi10Mg Alloy: A Comprehensive Analysis of Microstructure Evolution, Properties, and Future Prospects," Meta 13, no. 9 (2023): 1619.
5. Priya Sahadevan, Chithirai Pon Selvan, Manjunath Patel G C, Amiya Bhaumik (2023), Selective Laser Melting Process Parameter Optimization on Density and Corrosion Resistance of 17-4PH Stainless Steel, Archives of Foundry Engineering, ISSN (2299-2944), (4), pp. 105 – 116, DOI: 10.24425/afe.2023.146685.
6. Balbaa, M., & Elbestawi, M. A. (2021). Process parameter optimization for selective laser melting of Inconel 718. *Journal of Materials Processing Technology*, 295, 117167. https://doi.org/10.1016/j.jmatprotec.2021.117167
7. Tran, H.-C., Lo, Y.-L., Le, T.-N., Lau, A. K.-T., & Lin, H.-Y. (2022). Multi-scale simulation approach for identifying optimal parameters for fabrication of high-density Inconel 718 parts using selective laser melting. *Rapid Prototyping Journal*, 28(1), 109–125. https://doi.org/10.1108/RPJ-11-2020-0278

8. Elahi, S. M., Tavakoli, R., Boukellal, A. K., Isensee, T., Romero, I., & Tourret, D. (2022). Multiscale simulation of powder-bed fusion processing of metallic alloys. *Computational Materials Science*, 202, 110996. https://doi.org/10.1016/j.commatsci.2021.110996
9. Gallmeyer, T. G., Moorthy, S., Kappes, B. B., Mills, M. J., Stebner, A. P., & Aminahmadi, B. (2019). Knowledge of Process-Structure-Property Relationships to Engineer Better Heat Treatments for Laser Powder Bed Fusion Additive Manufactured Inconel 718. *Materials Science and Engineering: A*, 745, 1–11. https://doi.org/10.1016/j.msea.2018.12.084
10. Kladovasilakis, N., Charalampous, P., Tsongas, K., Kostavelis, I., Tzovaras, D., & Tzetzis, D. (2020). Influence of Selective Laser Melting Additive Manufacturing Parameters in Inconel 718 Superalloy. *Materials*, 13(20), 4555. https://doi.org/10.3390/ma13204555
11. Lu, C., & Shi, J. (2022). Relative density and surface roughness prediction for Inconel 718 by selective laser melting: central composite design and multi-objective optimization. *The International Journal of Advanced Manufacturing Technology*, 119(9–10), 3931–3949. https://doi.org/10.1007/s00170-021-08388-2
12. E. Yasa, "Selective Laser Melting: Principles and Surface Quality," in Additive Manufacturing (Elsevier, 2021), 77–120.
13. Balbaa, M., & Elbestawi, M. A. (2021). Process parameter optimization for selective laser melting of Inconel 718. *Journal of Materials Processing Technology*, 295, 117167. https://doi.org/10.1016/j.jmatprotec.2021.117167
14. Tran, H.-C., Lo, Y.-L., Le, T.-N., Lau, A. K.-T., & Lin, H.-Y. (2022). Multi-scale simulation approach for identifying optimal parameters for fabrication of high-density Inconel 718 parts using selective laser melting. *Rapid Prototyping Journal*, 28(1), 109–125. https://doi.org/10.1108/RPJ-11-2020-0278
15. Elahi, S. M., Tavakoli, R., Boukellal, A. K., Isensee, T., Romero, I., & Tourret, D. (2022). Multiscale simulation of powder-bed fusion processing of metallic alloys. *Computational Materials Science*, 202, 110996. https://doi.org/10.1016/j.commatsci.2021.110996
16. Gallmeyer, T. G., Moorthy, S., Kappes, B. B., Mills, M. J., Stebner, A. P., & Aminahmadi, B. (2019). Knowledge of Process-Structure-Property Relationships to Engineer Better Heat Treatments for Laser Powder Bed Fusion Additive Manufactured

Inconel 718. *Materials Science and Engineering: A*, 745, 1–11. https://doi.org/10.1016/j.msea.2018.12.084

17. Kladovasilakis, N., Charalampous, P., Tsongas, K., Kostavelis, I., Tzovaras, D., & Tzetzis, D. (2020). Influence of Selective Laser Melting Additive Manufacturing Parameters in Inconel 718 Superalloy. *Materials*, 13(20), 4555. https://doi.org/10.3390/ma13204555
18. Lu, C., & Shi, J. (2022). Relative density and surface roughness prediction for Inconel 718 by selective laser melting: central composite design and multi-objective optimization. *The International Journal of Advanced Manufacturing Technology*, 119(9–10), 3931–3949. https://doi.org/10.1007/s00170-021-08388-2
19. A. A. Okunkova, S. R. Shekhtman, A. S. Metel, et al., "On Defect Minimization Caused by Oxide Phase Formation in Laser Powder Bed Fusion," Meta 12, no. 5 (2022): 760.
20. Balbaa, M., & Elbestawi, M. A. (2021). Process parameter optimization for selective laser melting of Inconel 718. *Journal of Materials Processing Technology*, 295, 117167. https://doi.org/10.1016/j.jmatprotec.2021